Supplementary information

Heterojunction-engineered two-dimensional Ti_3C_2-$CoFe_2O_4$ nanozyme with oxidase-like activity for SERS detection of glutathione in human serum

Huiqi Zhu, [a] Ying Chen, [a] Weiqing Yang, [a] Zunxiang Zeng, [a] Yuling Hu *[a] and Ji Zhang *[b]

[a] *School of Chemistry, Institute of Green Chemistry and Molecular Engineering, Sun Yat-sen University, Guangzhou, 510006, China*
[b] *Department of Neurosurgery, State Key Laboratory of Oncology in Southern China, Sun Yat-sen University Cancer Center, Collaborative Innovation Center for Cancer Medicine, Guangzhou 510060, China*

This PDF file includes:

S1. Experimental sections

S1.1 *Steady-kinetic analysis*

The initial reaction rate V in the formula can be expressed by the generation rate of oxidized TMB (oxTMB), that is, the change rate of oxTMB absorption at 652 nm, which can be obtained from the Lambert-Beer law ($A = \varepsilon \cdot b \cdot c$) and the rate formula $V = A/(\varepsilon \cdot b \cdot \Delta t)$, where A is the measured absorbance of oxTMB, ε is the molar extinction coefficient of oxTMB, its value is 39,000 M^{-1} cm^{-1}, and b is the thickness of the liquid layer (the thickness of the cuvette used). From this, we can obtain a series of initial reaction rates V by changing the concentration of the reaction substrate [S]. The slope is K_m/V_{max} and the intersection of max of y-axis is $1/ V_{max}$.

S1.2 *LOD calculation*

The limit of detection was calculated using the formula: LOD = 3σ/slope, where σ represents the standard deviation of the blank and the slope is got from the fitting liner.

S1.3 *Detailed Calculation of Band Edge Positions for $CoFe_2O_4$*

According to Mott-Schottky (M-S) theory, the flat-band potential (E_{fb}) is obtained by extrapolating the tangent of the linear segment of the curve to $1/C^2 = 0$, where the intercept corresponds to E_{fb}. The M-S curve of $CoFe_2O_4$ (Fig. S7) shows a clear negative slope, confirming its p-type semiconductor characteristic with holes as the dominant carriers. Extrapolation of the linear segment yields an E_{fb} of 0.66 V vs. Ag/AgCl. Via the standard conversion formula ($E_{NHE} = E_{Ag/AgCl} + 0.197$ V), its E_{fb} relative to the normal hydrogen electrode (NHE) was calculated to be 0.86 V vs. NHE. It is generally known that the valence band potential (E_{VB}) of p-type semiconductors is very close to E_{fb} (about 0.10 V more positive)[1], so the E_{VB} of $CoFe_2O_4$ can be roughly deduced to be 0.96 V vs. NHE. Based on the UV-vis diffuse reflectance spectroscopy (DRS) Tauc plot of $CoFe_2O_4$ (Fig. S6), the band gap energy (E_g) was determined to be 1.39 eV. Using the relationship $E_{CB} = E_{VB} - E_g$ (where E_{CB} denotes the conduction band potential), the E_{CB} of $CoFe_2O_4$ was calculated to be -0.43 V vs. NHE. The Fermi level (E_f) of Ti_3C_2 is cited from the literature-reported DFT calculation result (E_f = -0.04 V vs. NHE)[2], and the E_f of p-type $CoFe_2O_4$ is well-documented to be closely aligned with its valence band. For the Ti_3C_2-$CoFe_2O_4$ Mott-Schottky junction, the Schottky barrier height (Φ_B) is $\Phi_B = E_{VB} - E_f = 1.00$ eV.

S1.4 *Preparation of $Ti_3C_2/CoFe_2O_4$ Physical-Mixture Series*

With 10 mg of Ti_3C_2 kept constant, 15 mg, 30 mg and 90 mg of $CoFe_2O_4$ were added separately. The mixtures were hand-ground in an agate mortar, dispersed in water at 1 mg mL^{-1}, and ultrasonicated for 30 minutes to afford the $Ti_3C_2/CoFe_2O_4$ physical-mixture series denoted as $Ti_3C_2/CoFe_2O_4$-1 physical mixture, $Ti_3C_2/CoFe_2O_4$-2 physical mixture and $Ti_3C_2/CoFe_2O_4$-3 physical mixture.

S2. Supporting Figures

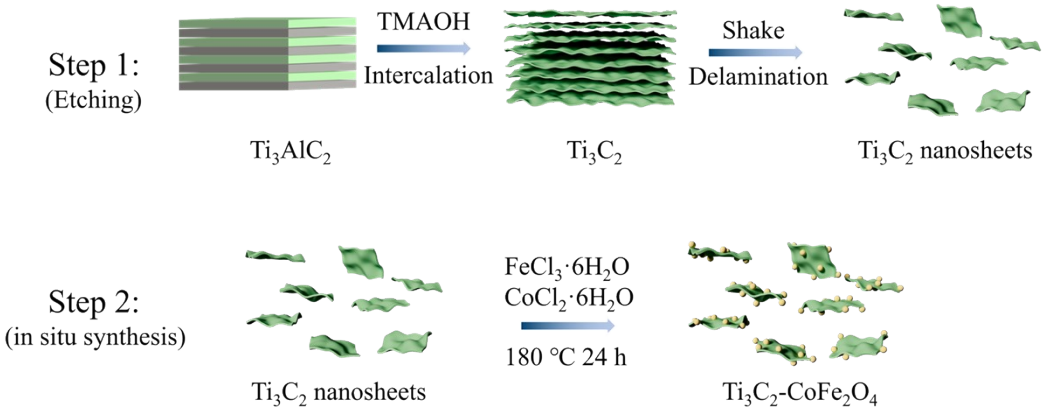

Scheme S1. The preparation procedure of the Ti_3C_2-$CoFe_2O_4$ composites.

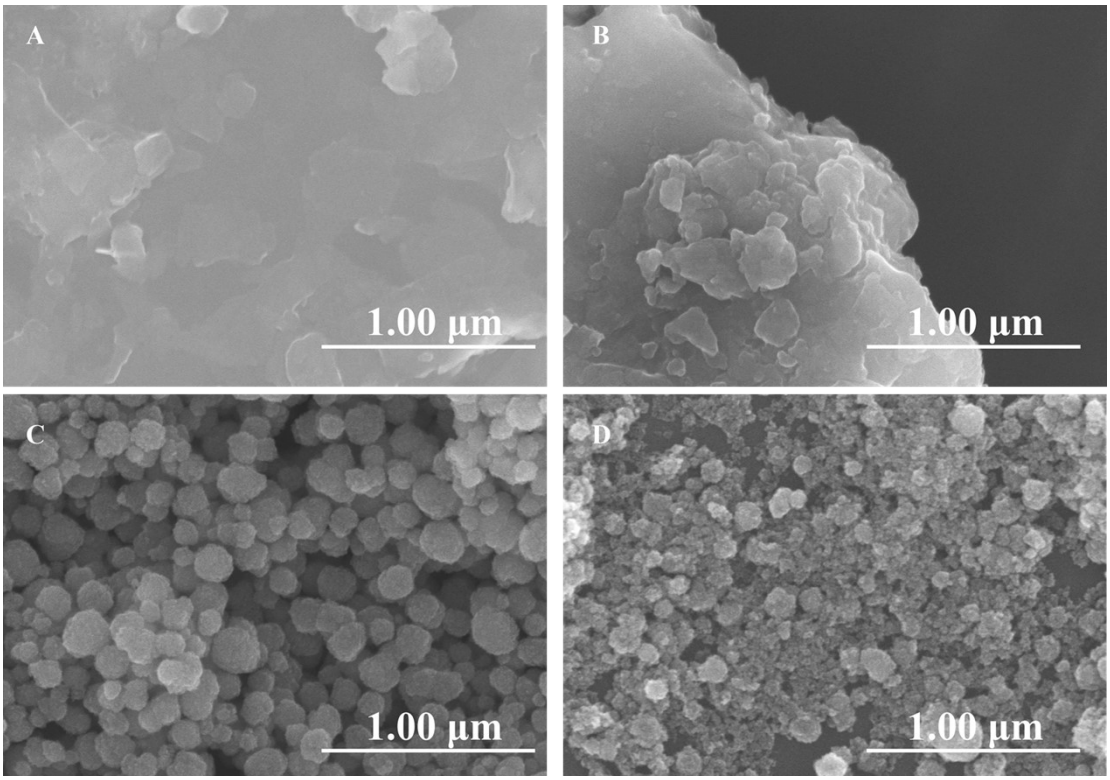

Fig. S1. SEM images of (A) Ti_3C_2 MXene, (B) Ti_3AlC_2, (C) $CoFe_2O_4$ and (D) Ti_3C_2-$CoFe_2O_4$.

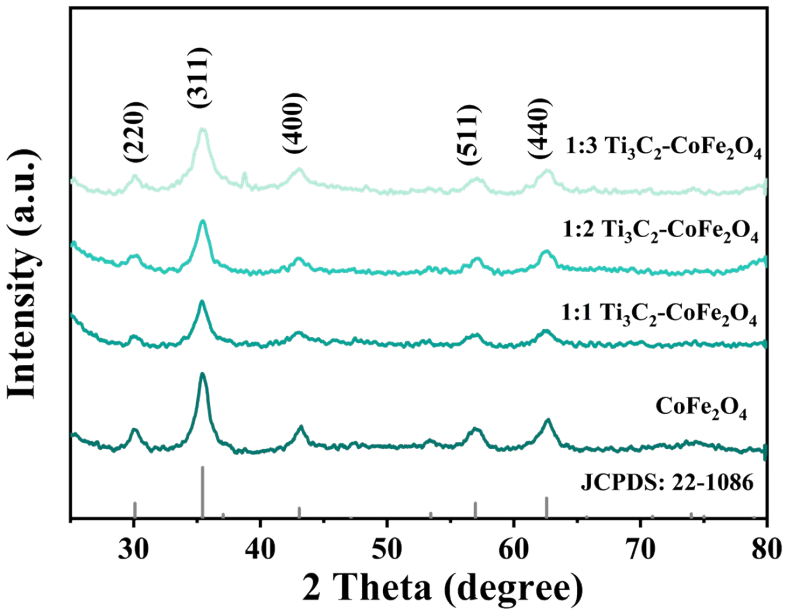

Fig. S2. XRD patterns of $CoFe_2O_4$ and Ti_3C_2-$CoFe_2O_4$ composites with different Ti_3C_2 MXene contents.

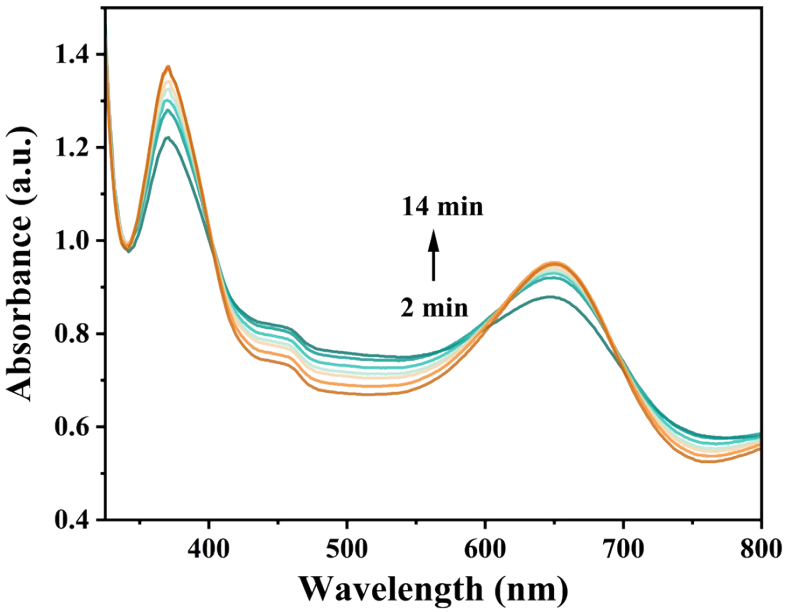

Fig. S3. UV-vis absorption spectra of TMB reaction solutions in the presence of Ti_3C_2-$CoFe_2O_4$.

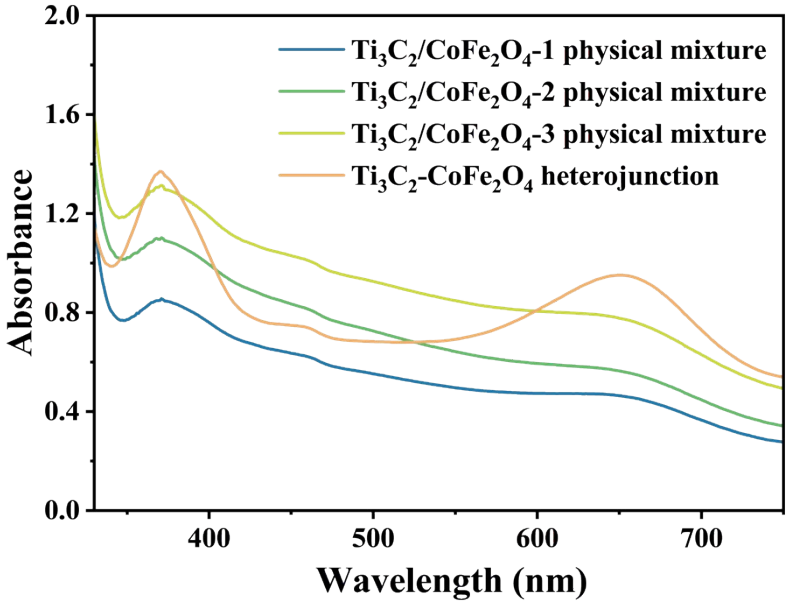

Fig. S4. UV-vis absorption spectra of TMB reaction solutions in the presence of Ti_3C_2-$CoFe_2O_4$ heterojunction, $Ti_3C_2/CoFe_2O_4$-1, $Ti_3C_2/CoFe_2O_4$-2 and $Ti_3C_2/CoFe_2O_4$-3 physical mixture.

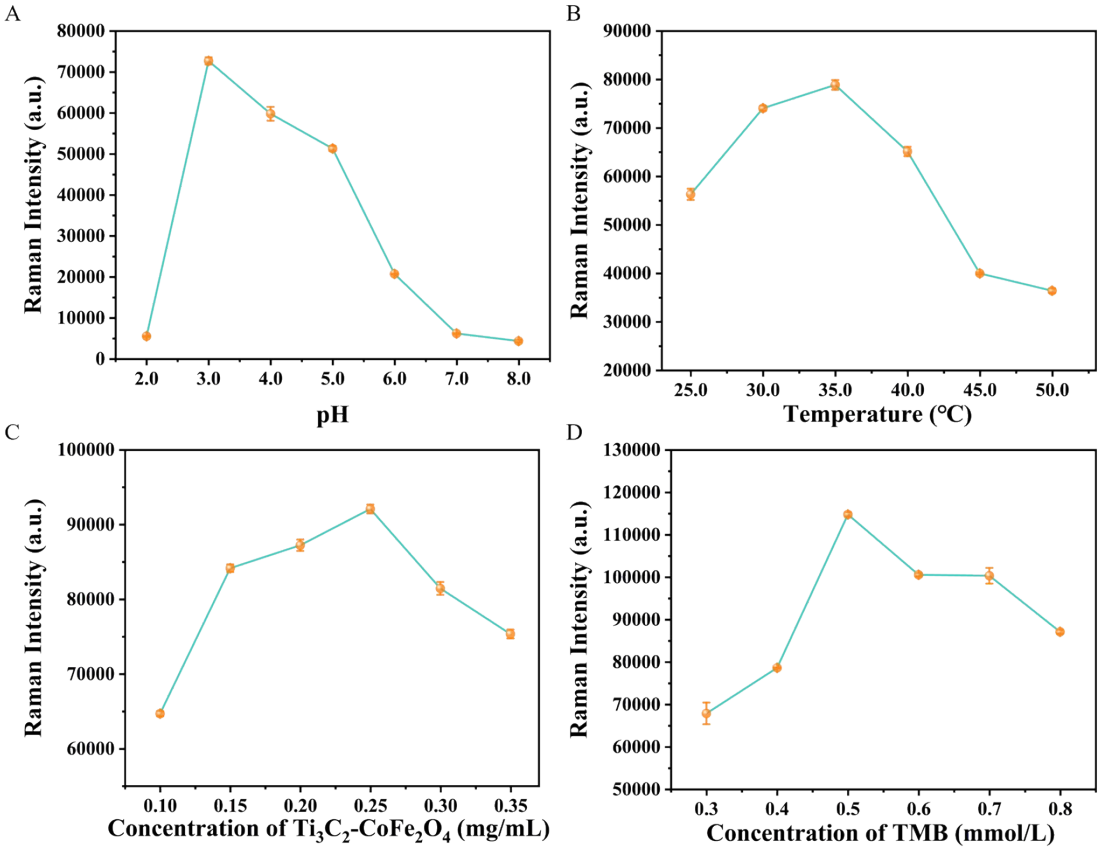

Fig. S5. The effect of (A) pH values, (B) temperatures, (C) Ti_3C_2-$CoFe_2O_4$ concentrations, and (D) TMB concentrations on the OXD-like activity of Ti_3C_2-$CoFe_2O_4$.

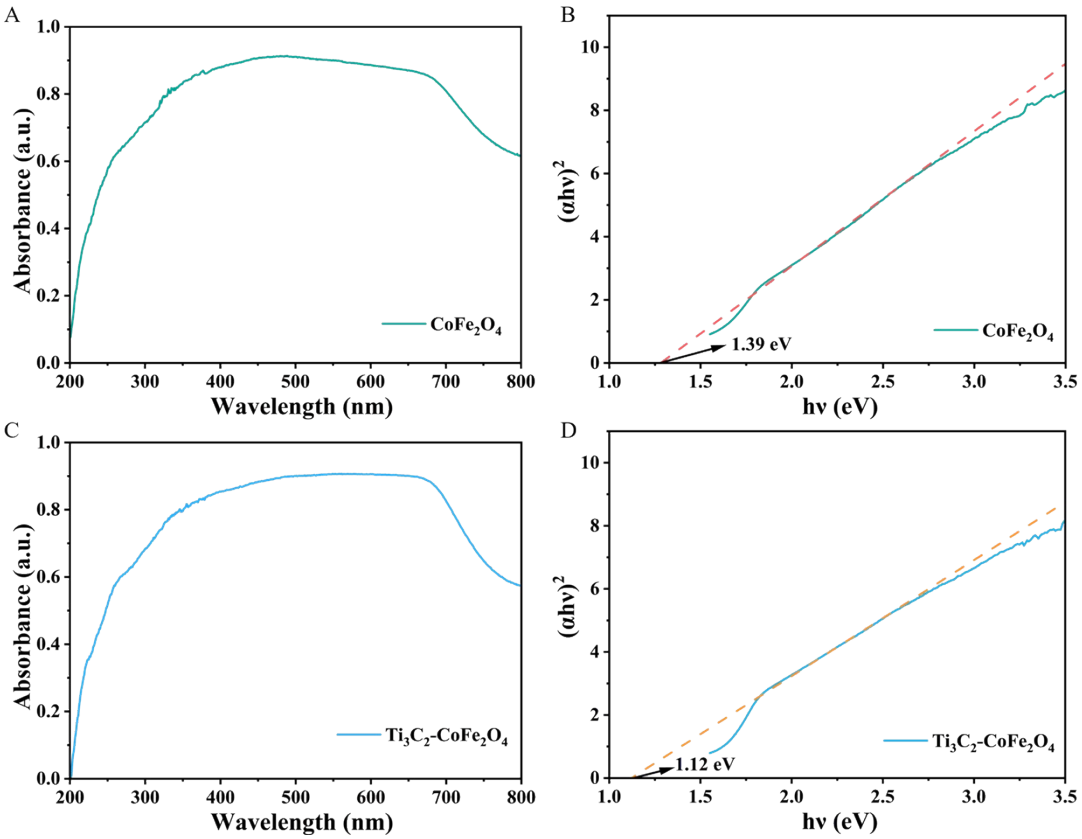

Fig. S6. UV-vis DRS spectra of (A) $CoFe_2O_4$ and (C) Ti_3C_2-$CoFe_2O_4$. Bandgaps of (B) $CoFe_2O_4$ and (D) Ti_3C_2-$CoFe_2O_4$.

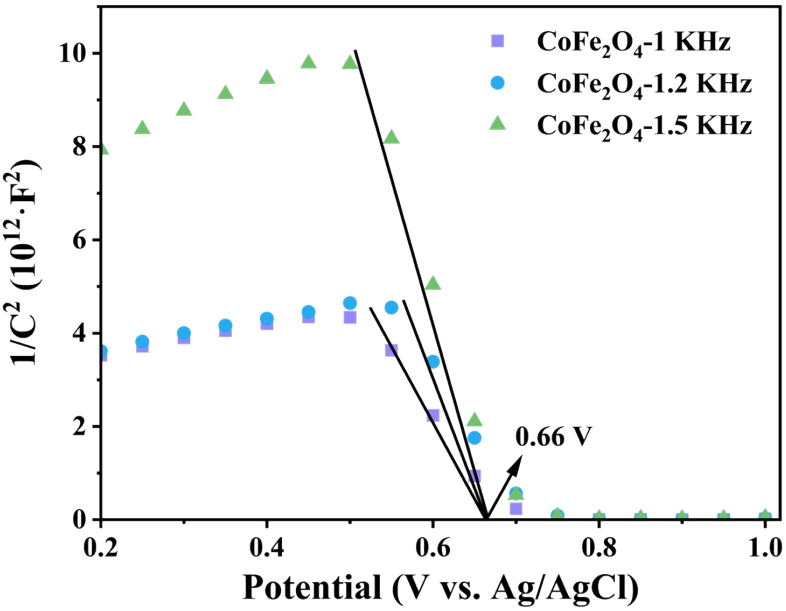

Fig. S7. M-S plot of $CoFe_2O_4$.

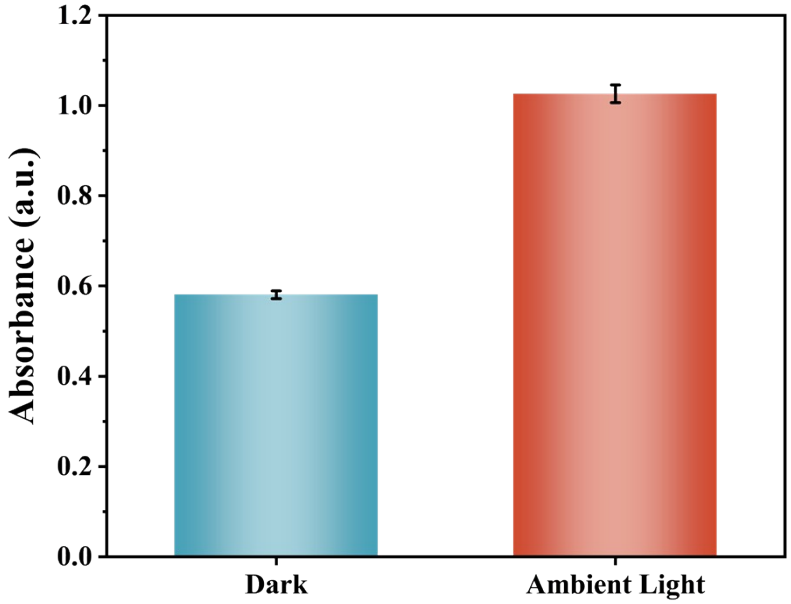

Fig. S8. UV-vis absorption intensity measured at 652 nm of oxTMB solutions in the presence of Ti_3C_2-$CoFe_2O_4$ under dark and ambient light conditions.

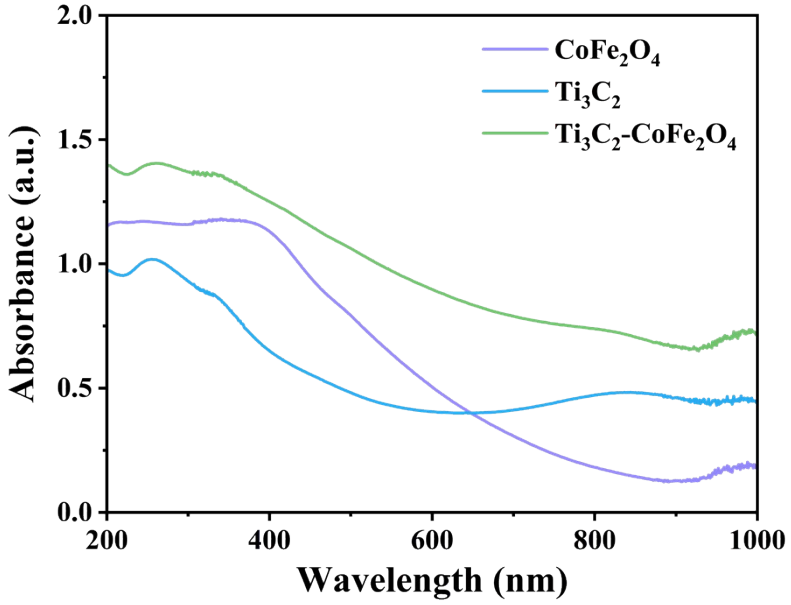

Fig. S9. UV-vis-NIR absorption spectra of $CoFe_2O_4$, Ti_3C_2, and Ti_3C_2-$CoFe_2O_4$.

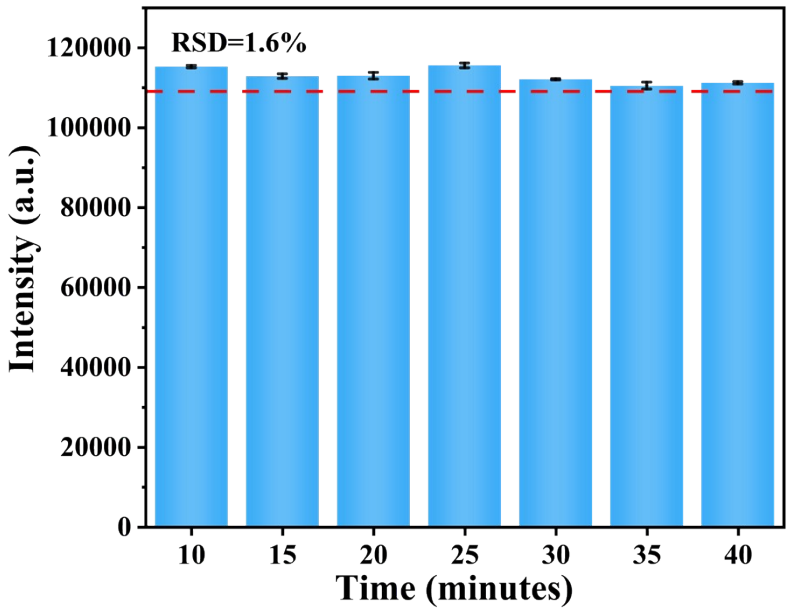

Fig. S10. Time-dependent SERS intensity of TMB (0.5 mmol/L) adsorbed on Ti_3C_2-$CoFe_2O_4$ composite at 1615 cm^{-1} (RSD = 1.6%).

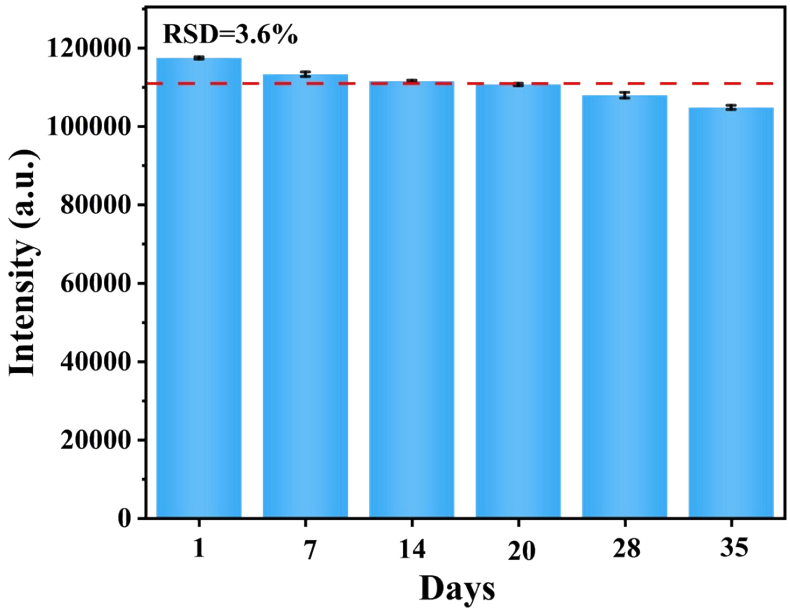

Fig. S11. The SERS intensity of TMB (0.5 mmol/L) with Ti_3C_2-$CoFe_2O_4$ at 1615 cm^{-1} for different days (RSD = 3.6%).

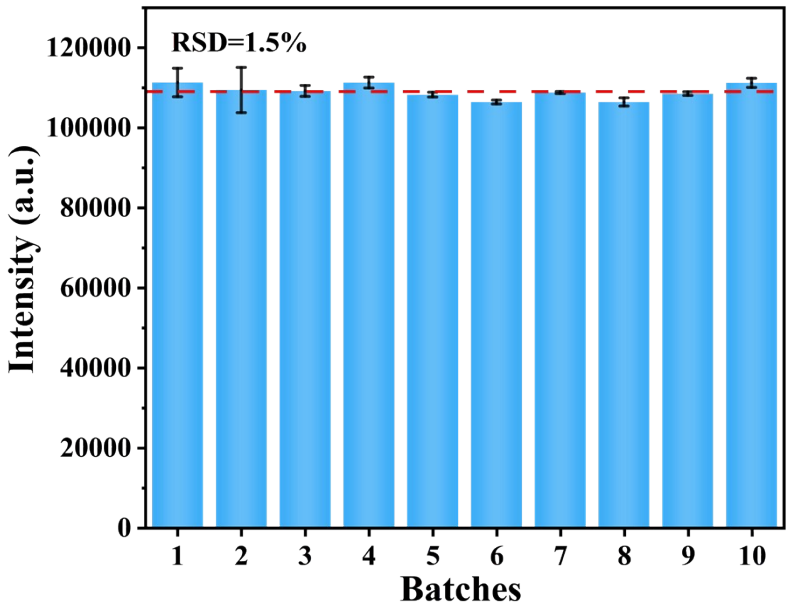

Fig. S12. The SERS intensity of TMB (0.5 mmol/L) with Ti_3C_2-$CoFe_2O_4$ at 1615 cm^{-1} for 10 different batches (RSD = 1.5%).

Table S1. Michaelis-Menten constant of TMB and its comparison with other nanozymes in the literature

Nanozyme	K_m (mM)	V_{max} (10^{-8} M/s)	Ref.
MNPC	0.159	20.5	(Gao et al., 2024) [3]
FeCo-NC	0.20	31.89	(Li et al., 2024) [4]
Fe-N-C SAzymes	1.81	0.0601	(Wu et al., 2019) [5]
CH-Cu	0.42	12.2	(Wang et al., 2019) [6]
Ti_3C_2-$CoFe_2O_4$	0.097	6.63	This work

Table S2. Comparison of the sensing performance with other methods in the detection of GSH.

Materials	Methods	Linear range (μmol/L)	LOD (μmol/L)	Ref.
Ti_3C_2/Pt ($M_{0.33}Pt$)	Colorimetry	0.4-7	0.0089	(Geng et al., 2022)[7]
MoS_2@$CoFe_2O_4$	Colorimetry	0.5-35	0.21	(Xian et al., 2021)[8]
$BaTiO_3$ NPs	Colorimetry	0.50-20	0.2	(Yang et al., 2023)[9]
Ti_3C_2 QDs	Fluorescence	1-100	0.02	(Xu et al., 2020)[10]
Mn:ZnS QDs@CNHs	Fluorescence	0.2-20	0.057	(Li et al., 2023)[11]
Au@MnO_2	SERS	0.5-30	0.1	(Wang et al., 2022)[12]
R-Fe_3O_4/Au	SERS	1-150	0.10	(Huang et al., 2022)[13]
HD-Pt@CeO_2	SERS	0.1-70	0.084	(Liao et al., 2024)[14]
Ti_3C_2-$CoFe_2O_4$	SERS	0.50-200	0.073	This work

Table S3. Detection of GSH concentration in human serum samples via SERS technology and Ellman's method (n = 3).

	GSH in clinical serum samples			
Samples	SERS method (μmol/L)	RSD (%, n =3)	Ellman's method (μmol/L)	Relative error
1	19.3	1.0	20.0	-3.4
2	30.0	5.0	30.0	-0.090
3	40.0	2.8	40.0	-0.74
4	57.2	6.4	55.0	4.1
5	29.1	1.2	30.0	-3.1
6	20.0	6.8	20.0	-0.24
7	14.2	3.7	15.0	-5.2
8	14.2	7.4	15.0	-5.5
9	45.3	9.7	45.0	0.65
10	48.0	3.7	50.0	-3.9

Note: Samples 1-5 were obtained from hepatocellular carcinoma patients collected at the Affiliated Cancer Hospital of Sun Yat-sen University; samples 6-10 were obtained from myocarditis patients at the Guangdong Second Provincial General Hospital.

S3. Supplementary References

1. Y. Jia, J. Yang, D. Zhao, H. Han and C. Li, *J. Energy Chem.*, 2014, **23**, 420-426.
2. J. Low, L. Zhang, T. Tong, B. Shen and J. Yu, *J. Catal.*, 2018, **361**, 255-266.
3. Y. Gao, J. Wang, L. Zhao, B. Yuan, Y. Kong, J. Luo, S. Zhao, W. Yang and R. Liu, *Food Chem.*, 2024, **441**, 138365.
4. Y. Li, Q. Ma, H. Gong, J. Gu, T. Liu and X. Wang, *Microchim. Acta*, 2024, **191**, 368.
5. Y. Wu, L. Jiao, X. Luo, W. Xu, X. Wei, H. Wang, H. Yan, W. Gu, B. Z. Xu, D. Du, Y. Lin and C. Zhu, *Small*, 2019, **15**, 1903108.
6. J. Wang, R. Huang, W. Qi, R. Su, B. P. Binks and Z. He, *Appl. Catal. B: Environ.*, 2019, **254**, 452-462.
7. H. Geng, Z. Li, Q. Liu, Q. Yang, H. Jia, Q. Chen, A. Zhou and W. He, *Dalton Trans.*, 2022, **51**, 11693-11702.
8. Z. Xian, L. Zhang, Y. Yu, B. Lin, Y. Wang, M. Guo and Y. Cao, *Microchim. Acta*, 2021, **188**, 65.
9. D. Yang, J. Liu, W. Hu, Y. Xiao, H. Chen, Y. Long and H. Zheng, *Sens. Actuators, B*, 2023, **393**, 134170.
10. X. Xu, H. Zhang, Q. Diao, Y. Zhu, G. Yang and B. Ma, *J. Mater. Sci.: Mater. Electron.*, 2020, **31**, 175-181.
11. X. Li, J. Qin and Y. Hu, *Microchem. J.*, 2023, **191**, 108763.
12. C. Wang, Y. Gao, S. Hu, A. Zhu, Y. Ying, X. Guo, Y. Wu, Y. Wen and H. Yang, *Biosens. Bioelectron.*, 2022, **215**, 114388.
13. Y. Huang, Y. Gu, X. Liu, T. Deng, S. Dai, J. Qu, G. Yang and L. Qu, *Biosens. Bioelectron.*, 2022, **209**, 114253.
14. Y. Liao, Y. He, B. Zhang, Y. Ma, M. Zhao, R. Xu and H. Cui, *Talanta*, 2024, **276**, 126234.